EBioMedicine 49 (2019) 331–340

Contents lists available at ScienceDirect

EBioMedicine

journal homepage: www.elsevier.com/locate/ebiom

Research paper

Uncoupling protein 1 inhibits mitochondrial reactive oxygen species generation and alleviates acute kidney injury

Ping Jia[a,e,1], Xiaoli Wu[b,1], Tianyi Pan[a,1], Sujuan Xu[a], Jiachang Hu[a], Xiaoqiang Ding[a,c,d,e,f,*]

[a] Division of Nephrology, Zhongshan Hospital, Fudan University, Shanghai, China
[b] Traditional Chinese Medicine Pharmacology Laboratory, Longhua Hospital, Shanghai University of Tranditional Chinese Medicine, Shanghai, China
[c] Shanghai Medical Center of Kidney, Shanghai, China
[d] Kidney and Dialysis Institute of Shanghai, Shanghai, China
[e] Kidney and Blood Purification Laboratory of Shanghai, Shanghai, China
[f] Hemodialysis quality control center of Shanghai, Shanghai, China

ARTICLE INFO

Article history:
Received 27 August 2019
Revised 5 October 2019
Accepted 14 October 2019
Available online 31 October 2019

Keywords:
Acute kidney injury
Uncoupling protein 1
Reactive oxygen species
Peroxisome proliferator-activator receptor γ

ABSTRACT

Background: Uncoupling protein 1 (UCP1) is predominantly found in brown adipose tissue mitochondria, and mediates energy dissipation to generate heat rather than ATP via functional mitochondrial uncoupling. However, little is known about its expression and function in kidney.

Methods: We carried out a mRNA microarray analysis in mice kidneys with ischemia reperfusion (IR) injury. The most dramatically downregulated gene UCP1 after IR was identified, and its role in generation of mitochondrial reactive oxygen species (ROS) and oxidative stress injury was assessed both in vitro and in vivo. Genetic deletion of UCP1 was used to investigate the effects of UCP1 on ischemia or cisplatin-indued acute kidney injury (AKI) in mice.

Findings: UCP1 was located in renal tubular epithelial cells in kidney and downregulated in a time-dependent manner during renal IR. Deletion of UCP1 increased oxidative stress in kidneys and aggravated ischemia or cisplatin induced AKI in mice.Viral-based overexpression of UCP1 reduced mitochondrial ROS generation and apoptosis in hypoxia-treated tubular epithelial cells. Furthermore, UCP1 expression was regulated by peroxisome proliferator-activator receptor (PPAR) γ in kidneys during renal IR. Overexpression of PPAR-γ resembled UCP1-overexpression phenotype in vitro. Treatment with PPAR-γ agonist could induce UCP1 upregulation and provide protective effect against renal IR injury in UCP1$^{+/+}$mice, but not in UCP1$^{-/-}$mice.

Interpretation: UCP1 protects against AKI likely by suppressing oxidative stress, and activation of UCP1 represents a potential therapeutic strategy for AKI.

Fund: National Natural Science Foundation of China grants, Science and Technology Commission of Shanghai.

1. Research in context

Evidence before this study: Uncoupling protein 1 (UCP1) is predominantly found in brown adipose tissue mitochondria, and has a central role in adaptive nonshivering thermogenesis in responsible to cold exposure via uncoupling ATP synthesis from respiration. Meanwhile, UCP1 may reduce reactive oxygen species generation in adipocyte mitochondria. However, little is known about its expression and function in kidney.

Added value of this study: In this study, using global gene expression profiling approach in a mouse model of renal ischemia reperfusion injury, we identify UCP1, which was the most downregulated gene in kidney 24 h after renal ischemia reperfusion, as a regulator of kidney injury, in particular regulation of reactive oxygen species generation and apoptosis. The results demonstrated that UCP1 reduced oxidative stress and alleviated ischemia or nephrotoxic drug-induced acute kidney injury (AKI)

Implications of all the available evidence: This study demonstrated the crucial role of PPAR-γ/UCP1 signaling pathway in regulating ischemia-induced oxidative stress and subsequent

* Corresponding author at: Division of Nephrology, Zhongshan Hospital, Fudan University, No. 180, Fenglin Road, Shanghai 200032, China.
E-mail address: ding.xiaoqiang@zs-hospital.sh.cn (X. Ding).
[1] PJ., X.W. and T.P. contributed equally to this work.

https://doi.org/10.1016/j.ebiom.2019.10.023

kidney injury, which is conducive to better understanding the pathogenesis of AKI. Activation of UCP1 may be a potential approach for prevention and treatment of AKI

2. Introduction

Acute kidney injury (AKI) is a common clinical complication characterised by the rapid loss of renal function, and is often caused by renal ischemia reperfusion (IR) and nephrotoxins in the clinics. Although supportive treatment is available, AKI is associated with high morbidity and mortality, and also contributes to the development of chronic kidney diseases [1]. Few specific therapies have emerged that can prevent or attenuate AKI. It is well known that AKI is a common reactive oxygen species (ROS)-related kidney disease [2]. The excess prodution of ROS and a reduction in antioxidant defenses are fundamentally implicated in the pathophysiology of AKI. During renal ischemia reperfusion injury (IRI), overproduction of ROS occurs early in the reperfusion phase and remains for 24 h after reperfusion [3]. ROS react with proteins, nucleic acids, carbohydrates and lipids, contribute to cell apoptosis and necrosis [4]. It has been demonstrated that the renal proximal tubular cells are particularly susceptible to the oxidative stress elicited by ischemia reperfusion-induced excess ROS [5]. Excess ROS impair the mitochondria, trigger inflammation and apoptosis [6]. Therefore, ROS are one of the critical targets in the management of AKI.

Mitochondria is the main source of ROS in cells [7]. A byproduct of mitochondrial respiration is a continual escape of electrons from the electron transport chain of the inner membrane which react directly with molecular oxygen to form ROS. Uncoupling proteins (UCPs), a family of mitochondrial anion carrier proteins expressed in the mitochondrial inner membrane, transport protons from inner membrane to the matrix, which causes a limited decrease in the inner membrane's potential, and thus reduces ROS emission from the electron transport chain, uncoupling respiration from ATP production [8]. While, when the mitochondrial permeability transition occurs, which is associated with the complete loss of the membrane potential, ROS burst is observed [9]. The first described UCP was UCP1 which was predominantly found in brown adipose tissue (BAT). UCP1 is critical for thermogenesis in responsible to cold exposure via uncoupling ATP synthesis from respiration and leading to heat production [10]. Moreover, several studies have demonstrated that UCP1 may reduce ROS generation by BAT mitochondria and thymus mitochondria [11–14].

In the present study, we carried out a mRNA microarray analysis in mice kidneys with IRI, and found UCP1 was the most downregulated gene. UCP1 was specificly located in the renal tubular epithelial cells in normal kidneys. Our in vivo studies together with in vitro experiments in which UCP1 was overexpressed or genetically deleted demonstrated the critical role of UCP1 in regulating the mitochondrial ROS generation and apoptosis associated with ischemia or hypoxic stress. Collectively, our data revealed that UCP1 may protect against AKI through inhibiting oxidative stress.

3. Materials and methods

3.1. Animals and animal experiments

Male C57BL/6 J mice were obtained commercially from the Animal Resource Center of Fudan University. UCP1$^{-/-}$ (129S-*Ucp1*^{tm1Kz}/J) mice were purchased from The Jackson Lab, backcrossed to C57B/6 J mice for 10 generations, and after repeated intercrossing UCP1$^{+/+}$ (wild type) and UCP1$^{-/-}$ strains were obtained and used for experiments. Adult (8- to 10-week-old) mice used in these experiments were housed in temperature- and humidity-controlled cages and fed a standard normal diet with free access to rodent food and water. All animal procedures in this study were approved by the Institutional Animal Care and Use Committee of Fudan University.

Renal IRI was induced by bilateral renal pedicle clamping for 30 min or 25 min (mild IRI), as described previously [15]. Sham-operated mice underwent the same surgical procedures but without occlusion of renal pedicle. Cisplatin-induced nephrotoxicity was induced by intraperitoneal injection with a single dose of cisplatin at 30 mg/kg, or 20 mg/kg (mild cisplatin challenge). To investigate the effects of PPAR-γ activation on AKI, we administered pioglitazone (Cayman Chemical, Ann Arbor, MI, USA) at a dose of 10 mg/kg/d, or the same volume of solvent, by oral gavage for seven consecutive days before IR surgery.

3.2. Cell culture and lentivirus transfection

Mouse renal tubular epithelial cells (mTECs) were purchased from Caltag Medsystems (Buckingham, UK), and cultured in Dulbecco's Modified Eagle's Medium supplemented with 10% fetal bovine serum, grown in incubators at 37 °C and 5% CO_2. For hypoxia, the cells were transferred to a hypoxia incubator with the desired level of hypoxia (2% O_2), and cultivated for 24 h.

Lentiviral vectors expressing UCP1 or PPAR-γ gene or enhanced green fluorescent protein (GFP) were constructed as described previously [16]. HEK293T cells were used to produce lentiviral particles by transfection of lentiviral expression vectors, pLV-CMV-STAT3,p80.9,pVSV-G, with pLentivirus-CMV-T2A-GFP, or pLentivirus-CMV-UCP1-T2A-GFP, or pLentivirus-CMV-PPAR-γ-T2A-GFP plasmids (for overexpression). Seventy-two hours after the transfection, the media containing lentiviruses were collected and incubated with mTECs for twenty-four hours.

3.3. Microarray hybridization

Total RNA from kidneys was extracted using Trizol reagent (Invitrogen, Carlsbad, USA) according to the manufacturer's instructions. Arraystar Mouse LncRNA Microarray V3.0 (KangChen Bio-technology Company, Shanghai, China) containing 35 923 LncRNA probes and 24 881 mRNA probes was used to detect the global profiling of mouse LncRNAs and mRNAs. Sample labeling and array hybridization were conducted according to the Agilent One-Color Microarray-Based Gene Expression Analysis protocol (Agilent Technology, USA).

3.4. Microarray data analysis

Agilent Feature Extraction software (version 11.0.1.1) was used to extract raw data and analyze acquired array images. GeneSpring GX v12.1 software package (Agilent Technologies, Santa Clara, CA, USA) was used to perform quantile normalization and subsequent data processing. Differentially expressed mRNAs with statistical significance in kidneys of wild-type mice between the sham group and IR group were identified through fold-change filtering (≥ 2.0), multiple hypothesis testing (FDR < 0.05), and unpaired t-tests ($p < 0.05$). Pathway analysis was performed to identify differentially regulated biological processes, based on KEGG (Kyoto Encyclopedia of Genes and Genomes). LncRNAs data was analyzed and further studied in another study. The microarray data have been deposited in NCBI Gene Expression Omnibus and are provided at: https://www.ncbi.nlm.nih.gov/geo/query/acc.cgi?acc=GSE131454. The accession number is GSE131454.

3.5. Human kidney tissue samples

We studied three normal controls and three patients with AKI in Zhongshan Hospital, Fudan University, between 2014 and 2018.

The control samples were from normal portions of nephrectomy specimens that had been removed for localized renal tumor, and verified by light microscopy. Acute tubular necrosis (ATN) was confirmed by renal biopsy in these patients with AKI. A ATN patient who had normal renal function before operation undergone surgery of ovarian tumor resection, accidental hemorrhage and hypotension occurred during the operation, serum creatinine was significantly increased 24 h after surgery. Two patients with ATN had a history of taking nephrotoxic drugs before onset. The renal biopsy tissues were subjected to immunohistochemistry staining. The study was approved by the Clinical Research Ethical Committee of the Zhongshan Hospital, Fudan University. All patients provided written informed consent.

3.6. Assessment of serum creatinine

Serum creatinine was determined in 100 µl of serum with an automated analyzer (Vet test 8008, USA).

3.7. Immunohistochemistry staining

Immunohistochemistry staining were performed as described previously [17]. The primary antibody was anti-UCP1 (ab209483, Abcam), and horseradish peroxidase-conjugated anti-rabbit IgG was used as secondary antibody. Images were visualized under light microscopy.

3.8. Immunofluorescence staining

Immunofluorescence staining was performed referring to the previously published method [18]. Anti-UCP1 (ab10983, Abcam) and FITC-labeled Lotus tetragonolobus lectin (FL-1321, Vector Laboratories, Burlingame, CA) were used as primary antibodies for frozen sections of mouse kidney. Secondary Alexa Fluor 555– or Alexa Fluor 488–conjugated antibodies against rabbit immunoglobulin (Invitrogen, Carlsbad, CA) were used to visualize antigen-antibody complexes. 4′, 6-diamidino-2 -phenylindole (DAPI) was used for nuclear staining. Images were recorded using a confocal microscope (Zeiss LSM 700, Germany).

3.9. ELISA of UCP1

Concentrations of UCP1 in blood and tissue homogenate were examined by commercially available ELISA kit (Wuhan Xinqidi Biological Technology, Inc., Wuhan, China), according to the manufacturer's protocol.

3.10. Examination of lipid peroxide

The level of malondialdehyde (MDA) in mouse renal tissue homogenate was tested using commercially available kit (TBARS Assay Kit, Cayman Chemical Company, USA), according to the manufacturer's protocol.

3.11. Flow cytometry

Cell apoptosis was detected by flow cytometric analysis with an Annexin V/PI kit (BD Bioscience, USA) according to the manufacturer's instructions. Cells with Annexin V (FITC) or propidium iodide (PI) staining or not were detected by flow cytometry (Beckman Coulter, CA, USA) and analyzed by FlowJo 7.6 software.

3.12. Mitochondrial ros generation assay

Cell mitochondrial ROS generation was detected using MitoSOX^{TM} Red mitochondrial superoxide indicator (Invitrogen) according to the manufacturer's instructions. Images were recorded by confocal microscopy. Tissue ROS production was detected on frozen kidney sections using Dihydroethidium (DHE) staining, as described previously [19]. Images were captured by confocal microscopy, and quantified morphometrically to measure area of fluorescent signal with Image-J.

3.13. Mitochondrial membrane potential assay with JC-1 staining

Mitochondrial membrane potential (MMP) assay kid (Beyotime, China) was used to detect MMP in mTECs according to the manufacturer's instructions. In healthy cells with high MMP, JC-1 enters mitochondria matrix, forming a polymer (j-aggregates) with intense red fluorescence. While, in unhealthy cells with low MMP, JC-1 remains as a monomer, shows only green fluorescence. Thus, MMP can be detected by the change of fluorescence color and analyzed by a flow cytometer. In brief, cells were collected and 500 μL JC-1 staining solution was added, and incubated for 20 min. Then cells were resuspended in 500 μL preheated JC-1 assay buffer, and analyzed using flow cytometer. Data are presented as mean of red/green fluorescence ratio.

3.14. Assessment of cell viability

Cell viability was determined by cell counting kit-8 (CCK8; Dojindo, Kumamoto, Japan) according to manufacturers' instructions. In brief, mTECss were treated with CCK-8 regent (100μL/well) and incubated for 2 h. The absorbance was measured at 450 nm with a microplate reader, and the cell viability was calculated.

3.15. Assessment of the activity of mitochondrial respiratory chain complex i/iii

The mitochondrial respiratory chain complex (MRCC) I/III kits (Solarbio, Beijing, China) were used to test the activity of MRCC I/III, as previously described [20]. In brief, 5×10^6 mTECs were homogenized on ice, centrifuged and the precipitant (mitochondria) was suspended, then treated by ultrasonication. The samples were mixed with working solution, and the initial absorbance (A1) and final absorbance after 2 min (A2) were recorded at 340 nm for MRCC I and at 550 nm for MRCC III, respectively. The activity of MRCC I/III was calculated.

3.16. Real-time polymerase chain reaction (PCR)

Total RNA from mTECs and dissected kidney tissue was extracted using Trizol reagent (Invitrogen, Carlsbad, CA), and then reverse-transcribed to complementary DNA (PrimeScript RT reagent Kit; TaKaRa, Japan), followed by real-time PCR (SYBR Premix Ex TaqTM TaKaRa). The PCR primer sequences were presented in Supplemental Table 1. The analysis method was as previously described [14].

3.17. Western blot

Western blot was performed as previously described [15]. The primary antibodies were used as follows: anti-UCP1 (ab209483, Abcam), anti-PPAR-γ (sc-7273, Santa Cruz Biotechnology), anti-Caspase 3 (#9662, Cell Signaling Technology) and anti-Cleaved Caspase 3 (#9661, Cell Signaling Technology), anti-GAPDH (sc-365,062, Santa Cruz Biotechnology).

3.18. Statistical analysis

Statistical analysis was performed using the SPSS Version 16.0 (Chicago, IL). Data were expressed as a mean ± SEM. The differences between two groups were analyzed by two-tailed, unpaired

t tests. For comparison of means among multiple groups, one-way ANOVA followed by Bonferroni posttest was applied. A P value less than 0.05 was determined to be significant.

4. Results

4.1. Renal ischemia reperfusion induces downregulation of UCP1

To systematically identify mRNAs involved in ischemic kidney injury, we used mRNA microarray to identify differentially expressed mRNAs during renal IR. The results showed that 267 mRNAs were differentially expressed after renal IR (fold change ≥2; $P < 0.05$), among which 192 were upregulated and 75 were downregulated. An expression volcano map of the differentially expressed mRNAs showed that UCP1 was most downregulated (Fig. 1A). Next, qRT-PCR was performed to analyze the expression of the top 11 downregulated mRNAs (fold change > 4) in the mouse kidneys 24 h after renal IR. The expression of most mRNAs was consistent with the microarray analysis except in the cases of NM_007702 and NM_009605, and NM_009463 (UCP1) was the most downregulated mRNA (Fig. 1B). Then, we detected the UCP1 expression in multiple organs in wild-type (WT) mice, and found it was specificly expressed in kidney, not in heart, liver and lung (Fig. 1C). While there was no expression of UCP1 in these organs in UCP1$^{-/-}$ mice (data not shown). UCP1 was present in the cytoplasm of tubular epithelial cells in both cortex and medulla of kidney (Fig. 1C). Furthermore, we examined the expression profiles of UCP1 mRNA during renal IR and found it was decreased in a time-dependent manner, and reached the lowest level at 24 h after renal IR (Fig. 1D). In the protein level, UCP1 was also downregulated after renal IR in kidneys and in the blood (Fig. 1E and Supplemental Fig. 1A,B).

In addition, we detected UCP1 expression in kidneys from patients with ATN caused by hemorrhage or nephrotoxic drugs, or normal controls. More detailed information about the patients and normal controls is available in the Materials and methods. Similarly, UCP1 was widely expressed in renal cortex and medulla of normal control kidneys, while, in kidneys of ATN patients, UCP1 expression was significantly downregulated (Fig. 1F).

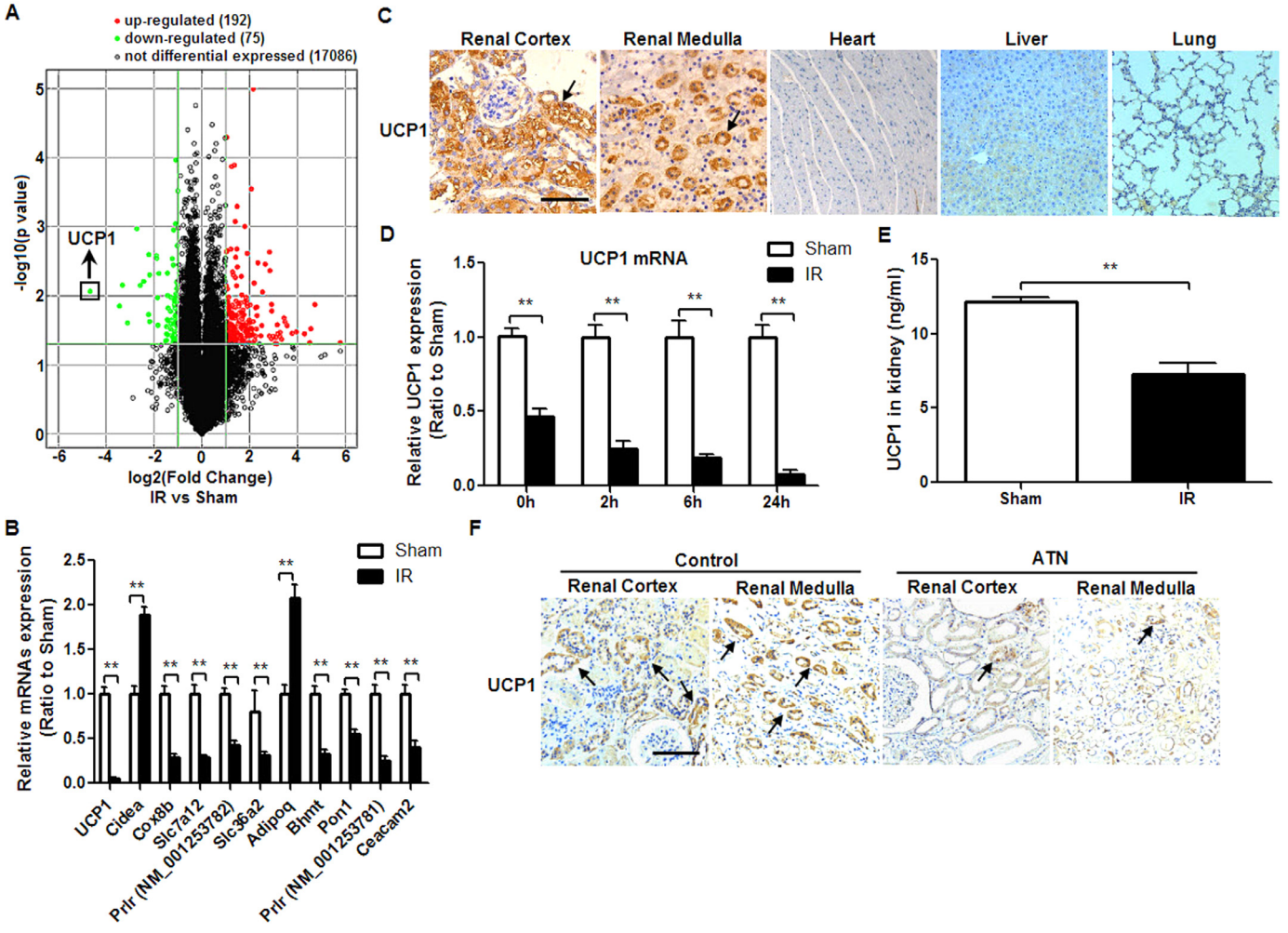

Fig. 1. Renal ischemia reperfusion (IR) induces downregulation of UCP1 in mice. (A) **A** volcano plot showed the differentially expressed mRNAs in IR group compared to Sham group. Red and green dots represent upregulated and downregulated mRNAs in kidneys 24 h after ischemia reperfusion (IR), respectively (fold change ≥2.0 and P-value ≤0.05). Black dots represent the genes that were not differentially expressed. UCP1 was the most downregulated gene. (B) Quantitative RT-PCR analysis of the top 11 downregulated mRNAs in the mouse kidneys 24 h after renal IR. (C) Immunohistochemical staining for UCP1 in multiple organs in mice. UCP1 was specificly expressed in kidney, including renal cortex and medulla (arrow). Scale bar, 100 μm. (D) Quantitative RT-PCR analysis of UCP1 mRNA during renal IR. (E) Enzyme-linked immunosorbent assay (ELISA) of UCP1 in kidney. Data represent mean ± SEM. $n = 4$–6. $^{**}P < 0.01$ versus Sham group. (F) Representative images of immunohistochemical staining for UCP1 in kidneys from patients with acute kidney injury (AKI) or normal controls. UCP1 was expressed in renal tubular epithelium (arrow). Scale bar, 100 μm. The control samples were from normal portions of nephrectomy specimens that had been removed for localized renal tumor. Acute tubular necrosis (ATN) was confirmed by renal biopsy in the patients with AKI.

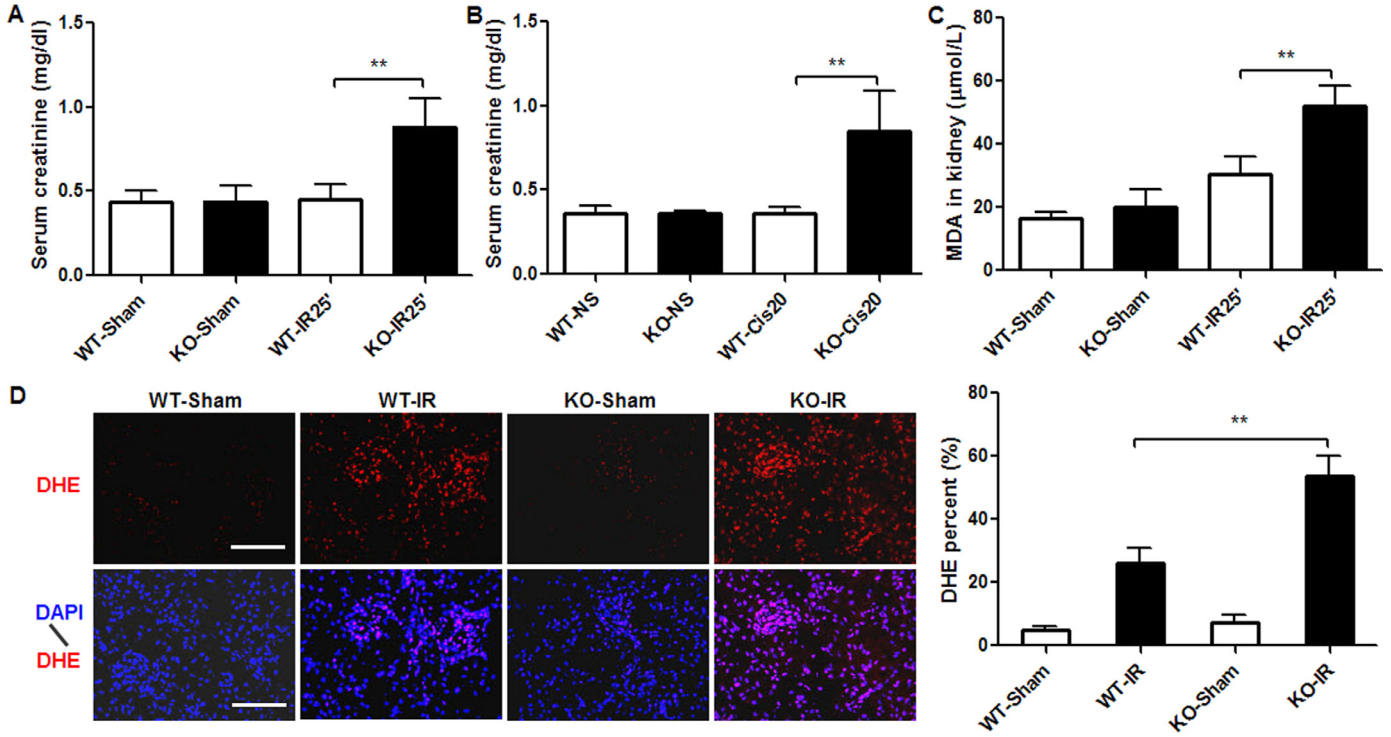

Fig. 2. Deletion of UCP1 aggravates acute kidney injury and increased reactive oxygen species generation. (A) Serum creatinine 24 h after renal IR. 25-min renal ischemia induced a significant increase in serum creatinine in UCP1$^{-/-}$ mice, but not in wild-type (WT) mice. (B) Serum creatinine 72 h after cisplatin injection. Treatment with 20 mg/kg cisplatin (Cis20) caused a significant increase in serum creatinine in UCP1$^{-/-}$ mice, but not in WT mice. (C) Malondialdehyde (MDA) concentration in mice kidneys. (D) Images and quantification of dihydroethidium (DHE) staining for detection of reactive oxygen species (ROS) generation in mice kidneys. Scale bar, 100 μm. Data represent mean ± SEM. $n = 6$. $^{*}P < 0.05$, $^{**}P < 0.01$ versus WT-IR25' or WT-Cis20' group.

4.2. Deletion of UCP1 aggravates acute kidney injury

To further determine the role of UCP1 in the pathogenesis of AKI, we subjected UCP1$^{-/-}$ mice and WT littermates to mild renal ischemia or a mild dose of cisplatin. The results showed that 25-minute clamping of bilateral renal pedicle did not cause an increase of serum creatinine 24 h after reperfusion in WT mice, while a significant increase of serum creatinine was found in UCP1$^{-/-}$ mice (Fig. 2A). Similarly, a mild single dose of cisplatin (20 mg/kg) caused a significant increase in serum creatinine in UCP1$^{-/-}$ mice, but not in WT mice (Fig. 2B). Next, we used DHE staining to assess the change in production of ROS, and found UCP1$^{-/-}$mice showed a higher production of ROS in kidney tissue 24 h after renal IR compared with WT mice (Fig. 2D). Meanwhile, the UCP1$^{-/-}$ mice had higher level of MDA in kidneys compared with WT mice (Fig. 2C). These results indicated that UCP1 could inhibit oxidative stress and conferred protective effects against AKI.

4.3. UCP1 overexpression reduces mitochondrial ros generation and apoptosis in hypoxia-treated tubular epithelial cells

To further investigate the effects of UCP1 overexpression on apoptosis and ROS generation in tubular epithelial cells treated with hypoxia, UCP1 was overexpressed in mTECs by transfection with UCP1 overexpressing lentivirus (UCP1-Lenti). Negative lentivirus (Neg-Lenti) was as control. The expression of UCP1 was significantly higher in mTECs infected with UCP1-Lenti than in that of Neg-Lenti (Supplemental Fig. 2A). We investigated the effects of UCP1 overexpression on mitochondria membrane potential (MMP) together with viability in mTECs. The results showed that UCP1 overexpression induced a mild decrease in MMP, while, did not affect cell viability (Supplemental Fig. 2B, C). Meanwhile, we examined the effects of UCP1 overexpression on mitochondria respiratory parameters, complex I and III, in mTECs. The results revealed that UCP1 overexpression did not affect the activity of mitochondria respiratory chain complex I and III (Supplemental Fig. 2D, E). As expected, overexpression of UCP1 significantly decreased mitochondrial ROS generation in mTECs treated with hypoxia, and also reduced apoptosis (Fig. 3A,C). Next, we examined the involvement of UCP1 overexpression in the expression of apoptosis-related protein caspase 3 in vitro. The results showed that the cleaved caspase 3 expression in mTECs transfected with UCP1-Lenti was significantly decreased compared to those transfected with Neg-Lenti in hypoxia (Supplemental Fig. 2F). In addition, we investigated the effect of UCP1 overexpression on mitochondrial membrane potential (MMP) in tubular epithelial cells treated with hypoxia. We found that the loss of MMP was significant in Hypoxia group. While, the MMP was significantly higher in UCP1 overexpression group than Hypoxia group (Fig. 3B).

4.4. PPAR-γ regulates UCP1 expression during renal ischemia reperfusion

Pathway analysis indicated that genes associated with PPAR signaling pathway were most downregulated by renal IR (Fig. 4A). It is well documented that the transcription of UCP1 is regulated by several key tissue-restricted transcription factors, including peroxisome proliferator-activator receptor (PPAR) α, γ, and PPAR-γ co-activator (PGC)−1α [21,22]. We detected the expression of PPARs in kidneys during IR. The results revealed that PPAR-α and PGC-1α mRNAs did not alter (Supplemental Fig. 3A,B), however, PPAR-γ mRNA was decreased in a time-dependent manner (Fig. 4B), which was consistent with the expression of UCP1 (Fig. 1D). Western blot analysis showed that both PPAR-γ and UCP1 were downregulated in kidneys 6 h and 24 h after renal IR (Supplemental Fig. 3C). In vitro, PPAR-γ and UCP1 proteins were

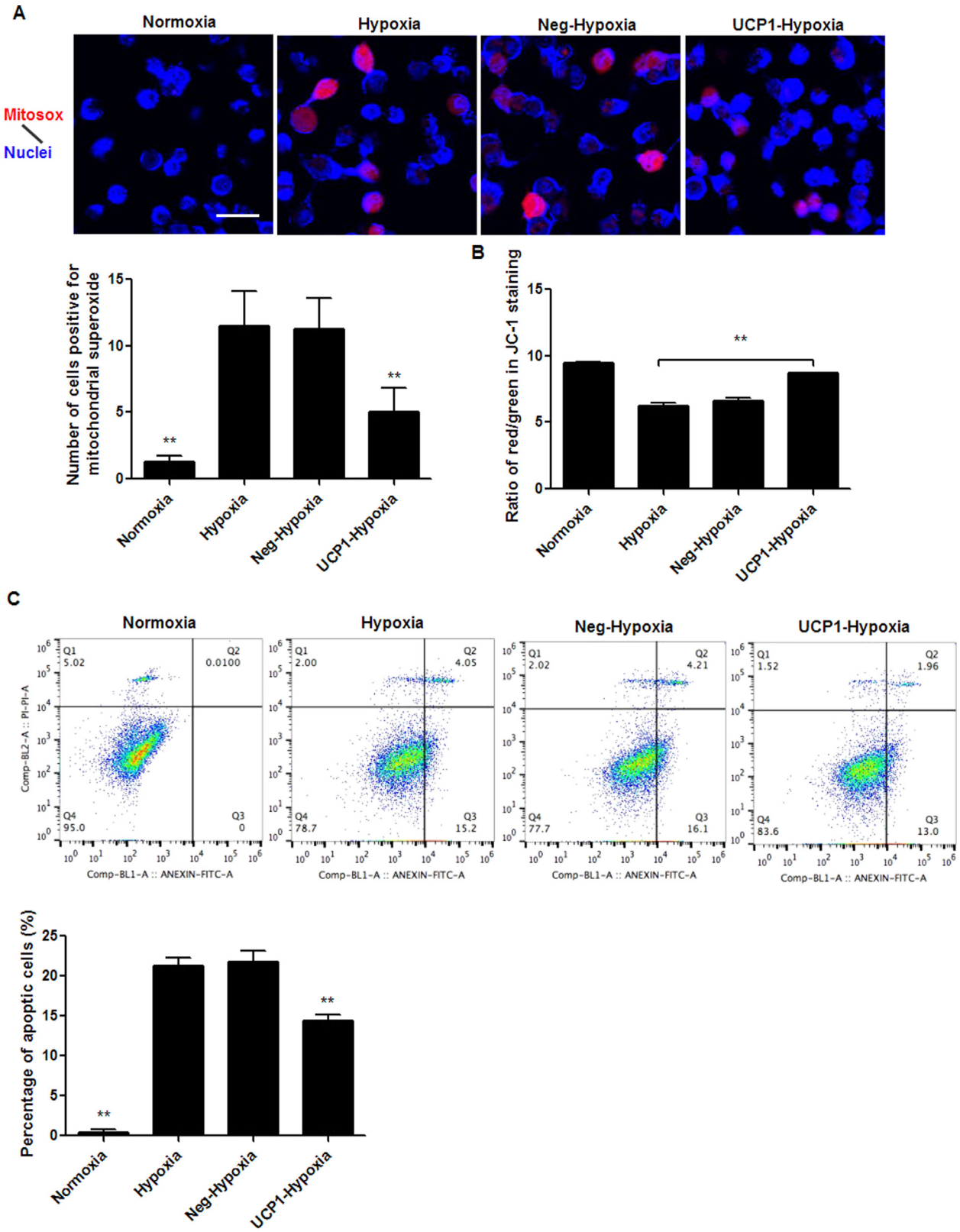

Fig. 3. UCP1 overexpression suppresses mitochondrial reactive oxygen species generation and apoptosis. (A) Images and quantification of mitochondrial reactive oxygen species (ROS) generation from hypoxia-treated mTEC transfected with UCP1 overexpressing lentivirus (UCP1-Hypoxia) or Negative lentivirus (Neg-Hypoxia). Scale bar, 25 μm. (B) Mitochondrial membrane potential was examined via JC-1 staining. Red inflorescence indicates the healthy mitochondria, and green inflorescence indicates the loss of mitochondrial potential. (C) Cell apoptosis in hypoxia-treated mTEC transfected with UCP1 overexpressing lentivirus or Negative lentivirus. The percentages of apoptotic cells were analyzed by Annexin V/PI analysis, and Annexin V positive cells were considered as apoptotic cells. Data represent mean ± SEM. $^{**}P < 0.01$ versus Hypoxia group.

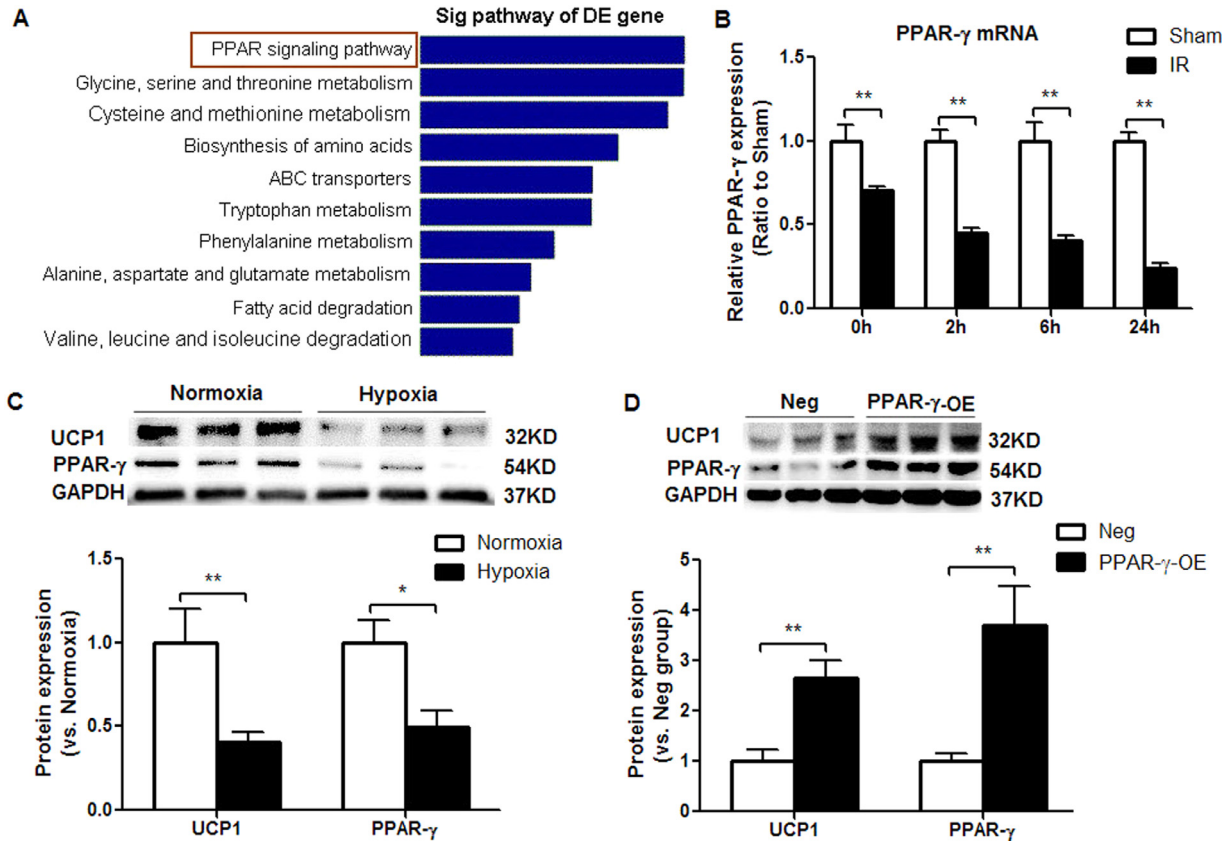

Fig. 4. PPAR-γ regulates UCP1 expression during renal ischemia reperfusion. (A) KEGG pathway enrichment analysis for downregulated mRNAs. Genes associated with PPAR signaling pathway were most downregulated 24 h after renal ischemia reperfusion (IR). (B) qRT-PCR analysis of PPAR-γ mRNA during renal IR in wild-type mice. Data represent mean ± SEM. $^{**}P < 0.01$ versus Sham group. (C) Western blot analysis of UCP1 and PPAR-γ in hypoxia-treated mTECs. (D) Western blot analysis of PPAR-γ and UCP1 in mTEC transfected with PPAR-γ overexpressing lentivirus (PPAR-γ-OE) or Negative lentivirus (Neg). PPAR-γ overexpression upregulated UCP1 expression. $^{*}P < 0.05$, $^{**}P < 0.01$. KEGG, Kyoto Encyclopedia of Genes and Genomes.

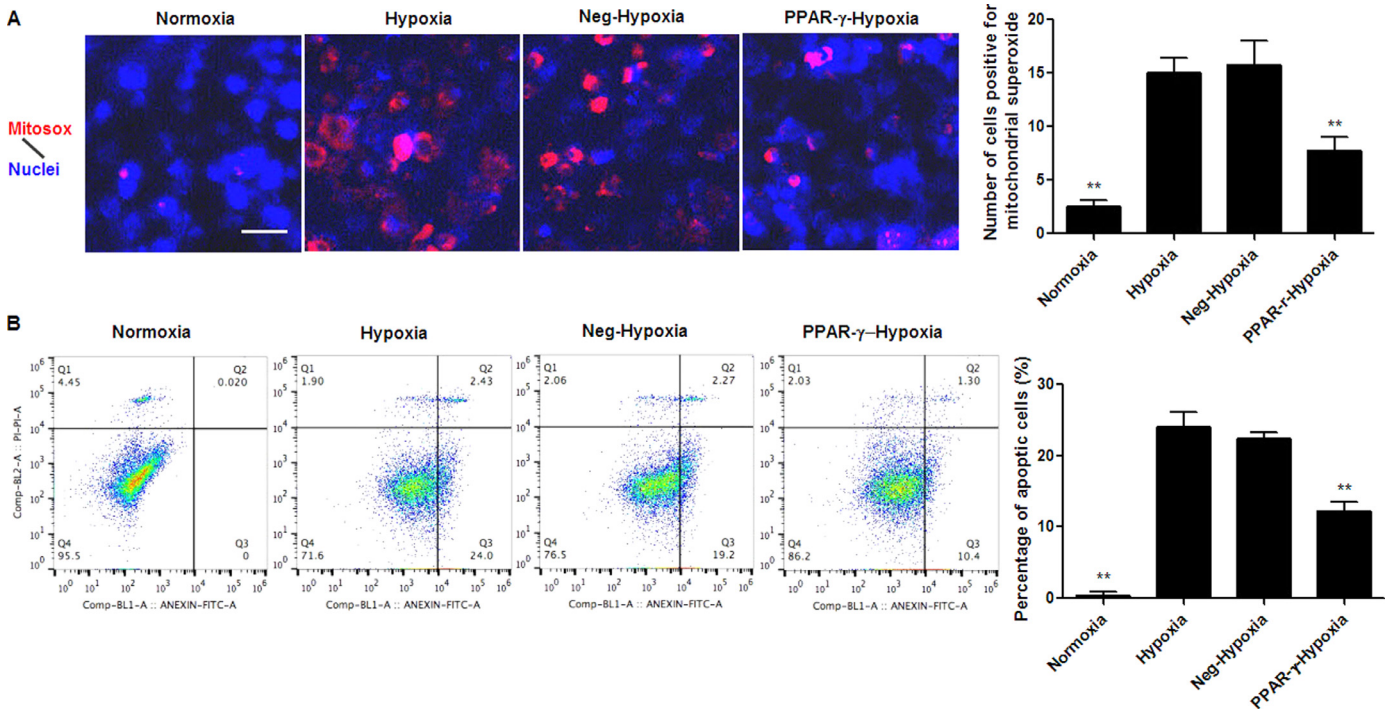

Fig. 5. PPAR-γ overexpression inhibites hypoxia-induced ROS generation and apoptosis in vitro. (A) Images and quantification of mitochondrial ROS generation from hypoxia-treated mTECs transfected with PPAR-γ overexpressing lentivirus (PPAR-γ-Hypoxia) or Negative lentivirus (Neg-Hypoxia). Scale bar, 25 μm. (B) Cell apoptosis in hypoxia-treated mTECs transfected with PPAR-γ overexpressing lentivirus or Negative lentivirus. The percentages of apoptotic cells were analyzed by Annexin V/PI analysis, and Annexin V positive cells were considered as apoptotic cells. $n = 4$. Data represent mean ± SEM. $^{**}P < 0.01$ versus Hypoxia group.

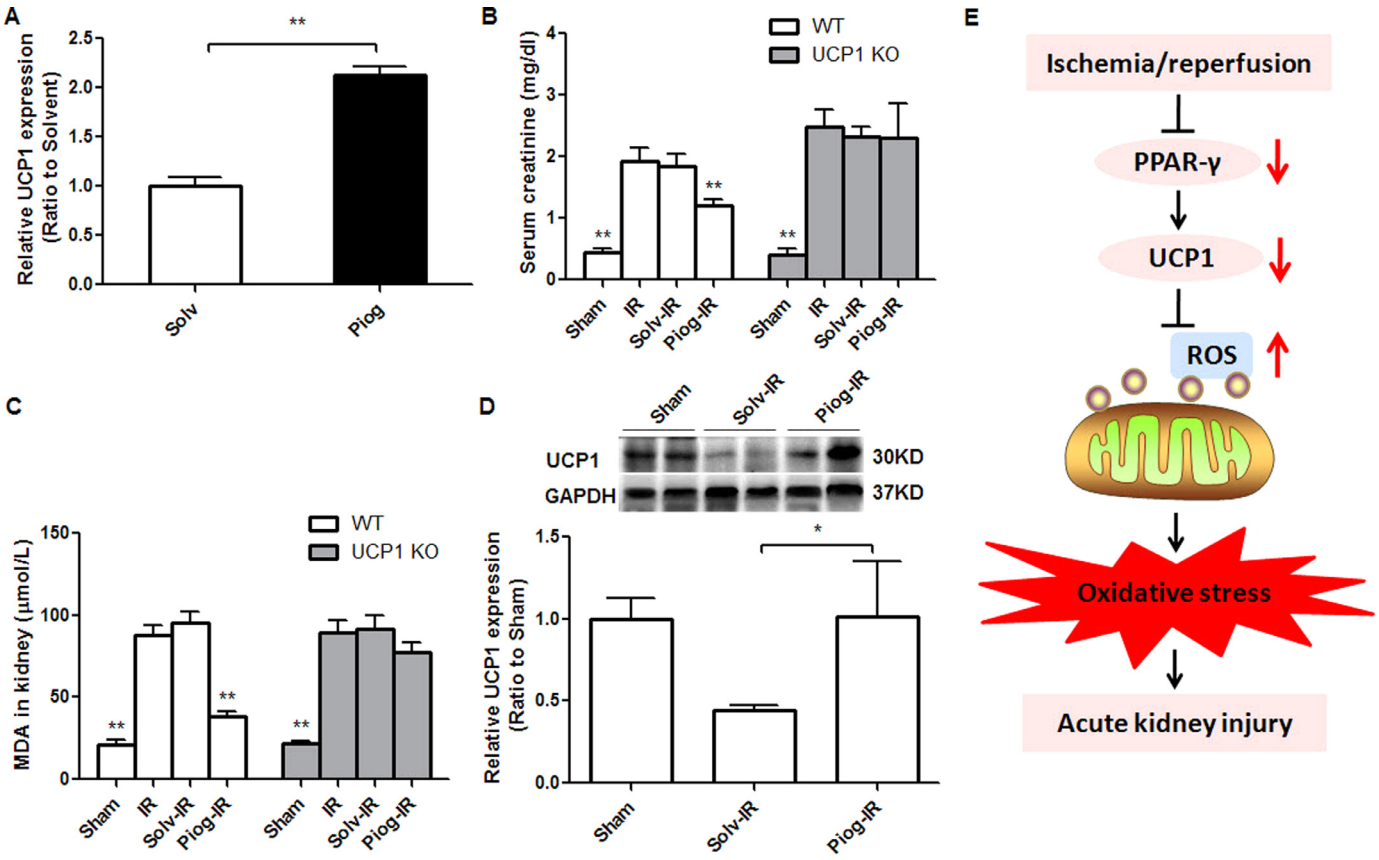

Fig. 6. PPAR-γ agonist upregulates UCP1 expression and attenuates ischemia-induced acute kidney injury and oxidative stress. (A) PPAR-γ agonist upregulated UCP1 mRNA expression in kidney. Mice were orally administered with PPAR-γ agonist pioglitazone (Piog, 10 mg / kg / day), or solvent (Solv) for one week. Data represent mean ± SEM. $n = 6$. $^{**}P < 0.01$. (B) Concentration of serum creatinine 24 h after renal ischemia reperfusion (IR). UCP1$^{-/-}$ (UCP1 KO) and wild-type (WT) mice were orally administered with PPAR-γ agonist pioglitazone or solvent for one week, and then subjected to renal IR. (C) Malondialdehyde (MDA) concentration in kidneys 24 h after renal IR in WT and UCP1$^{-/-}$ mice. Data represent mean ± SEM. $n = 6$. $^{**}P < 0.01$ versus IR group. (D) Western blot analysis of UCP1. Data are means from three independent experiments. $^{*}P < 0.05$. (E) Proposed schema of the pathway underlying renal ischemia reperfusion-induced acute kidney injury, involving downregulation of PPAR-γ and UCP1, promotion of mitochondrial reactive oxygen species (ROS) generation and oxidative stress.

also decreased in mTECs treated with hypoxia (Fig. 4C). We further examined the effect of PPAR-γ overexpression on the expression of UCP1 in mTECs. PPAR-γ was overexpressed in mTECs by transfection of PPAR-γ overexpressing lentivirus (Supplemental Fig. 4). As expected, overexpression of PPAR-γ significantly upregulated UCP1 expression (Fig. 4D). Collectively, these results suggested that UCP1 was regulated by PPAR-γ in kidney.

4.5. Overexpression of PPAR-γ inhibits hypoxia-induced ros generation and apoptosis in mTECs

We then investigated whether overexpression of PPAR-γ resembled UCP1-overexpression phenotype in vitro. PPAR-γ was overexpressed in mTECs by transfection with PPAR-γ overexpressing lentivirus (PPAR-γ-Lenti). Negative lentivirus (Neg-Lenti) was as control. Similarly, overexpression of the PPAR-γ significantly decreased mitochondrial ROS generation in mTECs treated with hypoxia, and also reduced apoptosis (Fig. 5A,B).

4.6. PPAR-γ agonist alleviates renal ischemia reperfusion injury via UCP1

Previous studies demonstrated that chronic treatment of PPAR-γ agonist could induce UCP1 upregulation in BAT and white adipose tissue [23,24]. Then, we investigated the effect of PPAR-γ agonist on the expression of UCP1 in kidney. Mice were orally administered with pioglitazone (10 mg / kg / day), a selective PPAR-γ agonist, or solvent for one week. The result revealed that PPAR-γ activation significantly upregulated UCP1 mRNA expression in kidney (Fig. 6A). Next, we examined whether PPAR-γ activation would provide protective effect against renal IRI and whether this effect was mediated by UCP1. UCP1$^{-/-}$ and WT mice were orally administered with pioglitazone or solvent for one week, and then subjected to renal IR. The results revealed that pioglitazone administration markedly reduced concentration of serum creatinine when compared to solvent administration in WT mice, but not in UCP1$^{-/-}$ mice (Fig. 6B). Moreover, pioglitazone administration caused a significant decrease in MDA in kidneys of WT mice when compared with that of UCP1$^{-/-}$ mice (Fig. 6C). Furthermore, pioglitazone administration upregulated UCP1 expression in kidneys in WT mice (Fig. 6D). These data indicated that PPAR-γ alleviated renal IRI via upregulation of UCP1.

5. Discussion

In this study, using global gene expression profiling approach in a mouse model of renal IRI, we identified UCP1 as a regulator of kidney injury, in particular regulation of ROS generation and inhibition of apoptosis. Renal ischemia induced downregulation of PPAR-γ, which inhibited UCP1 expression, and subsequently promoted mitochondrial ROS generation, resulting in oxidative stress injury and AKI (Fig. 6E). Moreover, deletion of UCP1 increased the generation of ROS, displayed greater susceptibility to renal IRI or

nephrotoxicity. As such, activation of UCP1 represents an approach for new therapeutics to treat AKI.

As mentioned above, UCPs play an important role in the generation of mitochondrial ROS. There are five UCPs (UCP-1 to −5) which are somewhat different in tissue distributions and functions. As the first identified and most studied uncoupling protein, UCP1 function and its expression have been highly contentious. Previous evidences suggested that UCP1 expression was limited to fat tissues [25,26], most abundant in the BAT. Here, we found UCP1 was also expressed in normal kidney, with widespread expression in the renal tubules (Fig. 1C and Fig. 1F), but not in heart, liver and lung. Early evidences showed that UCP1 had no effect on ROS generation and other markers of oxidative stress [27]. However, growing evidences have demonstrated that UCP1 activation may reduce mitochondrial ROS generation in BAT, beige adipose tissue, thymus and skeletal muscle [11–13,28]. Consistent with these results, our data indicated that UCP1 significantly reduced mitochondrial ROS generation in hypoxia-treated mTECs and ROS generation in ischemic kidneys from UCP1$^{-/-}$ mice was significantly higher than that from WT mice. UCP2 has high similarity with UCP1 in sequence, and is widely expressed in several tissues including kidney, heart, lung, and spleen [29–31]). In this study, our data indicated that UCP2 was upregulated in kidneys 24 h after IR (Supplemental Fig. 5), which was consistent with previous studies [32]. Upregulation of UCP2 could provide protective effects against renal IRI [32].

It is noteworthy that mitochondrial uncoupling induced by UCP1 causes a reduction in the oxidative phosphorylation, affecting the ATP production which is particularly important for proximal tubule epithelial cells to maintain cellular function. Whether mitochondrial uncoupling compromise the excretion and reabsorption process of tubular epithelia cells are not explored in this study. Recent evidence has indicated that the induction of mitochondrial uncoupling not only impacts mitochondrial respiration but also regulates multiple cellular biological processes, including autophagy, ROS production, protein secretion, physical exercise capacity [33–36]. Further experiments would be needed to elaborate these and improve our knowledge of the cellular consequences of mitochondrial uncoupling in resident kidney cells.

It has been demonstrated that the transcription of UCPs are regulated by PPAR-α, γ, and PGC-1α [37]. In vivo PPAR-γ activation can induce expression of UCP-1, −2, and −3 in BAT [21,23,38]. In the current study, pathway analysis indicated that genes associated with PPAR signaling pathway were most downregulated during renal IR (Fig. 4A), and we found that PPAR-γ mRNA was decreased consistent with the expression of UCP1 (Fig. 4B and Fig. 1D). Given the potential of PPAR-γ for regulation of UCP-1 expression, and that PPAR-γ acts as a regulator of energy homeostasis, we assessed the effects of PPAR-γ activation on UCP1 expression in kidneys, oxidative stress and renal damage induced by renal IR. Interestingly, we discovered that mice treated with pioglitazone, a selective PPAR-γ agonist, exhibited higher level of UCP1 protein in kidneys, lower MDA and attenuated renal injury, compared with the solvent control group mice. However, administration of pioglitazone did not attenuate oxidative stress and renal injury in UCP1$^{-/-}$ mice. It suggests that PPAR-γ activation may be associated with UCP1-mediated inhibition of oxidative stress and subsequent improvement of renal IRI.

In this study, PPAR-γ agonist (pioglitazone) was administered before the onset of renal injury, which is sort of limitation to perform in clinic. Nevertheless, in fact, it is possible to identify patients at high risk of AKI, such as major surgical procedures, severe infection, nephrotoxic drugs administration, especially in critically ill patients. Pre-activation of UCP1 may be beneficial for prevention of AKI.

The present study demonstrated the involvement of UCP1 in the beneficial response to AKI via inhibiting oxidative stress and apoptosis. PPAR-γ agonist provided protective effects against renal IRI through activation of UCP1. Further experimental studies and clinical trials would be valuable in insight into activation of UCP1 and its clinical application.

Author contributions

P.J. and X.D. designed the study; P.J., T.P., X.W., S.X. and J.H. carried out experiments; P.J., X.W, X.D., and T.P. analyzed the data; P.J., X.D. wrote the manuscript.

Declaration of Competing Interest

The authors declare that they have no conflict of interest.

Acknowledgments

This work was supported by the National Natural Science Foundation of China grants 81870466 (to Ping Jia), 81430015 and 81670614 (to Xiaoqiang Ding), Science and Technology Commission of Shanghai (14DZ2260200).

Supplementary materials

Supplementary material associated with this article can be found, in the online version, at doi:10.1016/j.ebiom.2019.10.023.

References

[1] Bellomo R, Kellum JA, Ronco C. Acute kidney injury. Lancet 2012;380:756–66.
[2] Plotnikov EY, Kazachenko AV, Vyssokikh MY, Vasileva AK, Tcvirkun DV, Isaev NK, et al. The role of mitochondria in oxidative and nitrosative stress during ischemia/reperfusion in the rat kidney. Kidney Int 2007;72(12):1493–502.
[3] Liang HL, Hilton G, Mortensen J, Regner K, Johnson CP, Nilakantan V. MnTMPyP, a cell-permeant sod mimetic, reduces oxidative stress and apoptosis following renal ischemia-reperfusion. Am J Physiol Renal Physiol 2009;296(2):F266–76.
[4] Bonventre JV, Weinberg JM. Recent advances in the pathophysiology of ischemic acute renal failure. J Am Soc Nephrol 2003;14(8):2199–210.
[5] Chatterjee PK, Cuzzocrea S, Brown PA, Zacharowski K, Stewart KN, Mota-Filipe H, et al. Tempol, a membrane-permeable radical scavenger, reduces oxidant stress-mediated renal dysfunction and injury in the rat. Kidney Int 2000;58(2):658–73.
[6] Hüttemann M, Helling S, Sanderson TH, Sinkler C, Samavati L, Mahapatra G, et al. Regulation of mitochondrial respiration and apoptosis through cell signaling: cytochrome c oxidase and cytochrome c in ischemia/reperfusion injury and inflammation. Biochim Biophys Acta 2012;1817(4):598–609.
[7] Mailloux RJ, Harper ME. Uncoupling proteins and the control of mitochondrial reactive oxygen species production. Free Radic Biol Med 2011;51(6):1106–15.
[8] Skulachev VP. Role of uncoupled and non-coupled oxidations in maintenance of safely low levels of oxygen and its one-electron reductants. Q Rev Biophys 1996;29(2):169–202.
[9] Zorov DB, Filburn CR, Klotz LO, Zweier JL, Sollott SJ. Reactive oxygen species (ROS)-induced ros release: a new phenomenon accompanying induction of the mitochondrial permeability transition in cardiac myocytes. J Exp Med 2000;192:1001–14.
[10] Fedorenko A, Lishko PV, Kirichok Y. Mechanism of fatty-acid-dependent UCP1 uncoupling in brown fat mitochondria. Cell 2012;151(2):400–13.
[11] Dlasková A, Clarke KJ, Porter RK. The role of ucp 1 in production of reactive oxygen species by mitochondria isolated from brown adipose tissue. Biochim Biophys Acta 2010;1797(8):1470–6.
[12] Oelkrug R, Kutschke M, Meyer CW, Heldmaier G, Jastroch M. Uncoupling protein 1 decreases superoxide production in brown adipose tissue mitochondria. J Biol Chem 2010;285(29):21961–8.
[13] Ježek P, Jabůrek M, Porter RK. Uncoupling mechanism and redox regulation of mitochondrial uncoupling protein 1 (UCP1). Biochim Biophys Acta Bioenerg 2019;1860(3):259–69.
[14] Clarke KJ, Porter RK. Uncoupling protein 1 dependent reactive oxygen species production by thymus mitochondria. Int J Biochem Cell Biol 2013;45(1):81–9.
[15] Jia P, Teng J, Zou J, Fang y, Zhang x, Bosnjak ZJ, et al. miR-21 contributes to xenon-conferred amelioration of renal ischemia-reperfusion injury in mice. Anesthesiology 2013;119(3):621–30.
[16] Tiscornia G, Singer O, Verma IM. Production and purification of lentiviral vectors. Nat Protoc 2006;1(1):241–5.
[17] Jia P, Teng J, Zou J, Fang Y, Wu X, Liang M, et al. Xenon protects against septic acute kidney injury via miR-21 target signaling pathway. Crit Care Med 2015;43(7):e250–9.

[18] Jung YJ, Lee AS, Nguyen-Thanh T, Kim D, Kang KP, Lee S, et al. SIRT2 regulates LPS-induced renal tubular CXCL2 and CCL2 expression. J Am Soc Nephrol 2015;26(7):1549–60.
[19] Gomez IG, MacKenna DA, Johnson BG, Kaimal V, Roach AM, Ren S, et al. Anti-microRNA-21 oligonucleotides prevent alport nephropathy progression by stimulating metabolic pathways. J Clin Invest 2015;125:141–56.
[20] Jin F, Wu Z, Hu X, Zhang J, Gao Z, Han X, et al. The PI3K/Akt/GSK-3β/ROS/eIF2B pathway promotes breast cancer growth and metastasis via suppression of nk cell cytotoxicity and tumor cell susceptibility. Cancer Biol Med 2019;16:38–54.
[21] Chen HY, Liu Q, Salter AM, Lomax MA. Synergism between cAMP and PPARγ signalling in the initiation of UCP1 gene expression in hib1b brown adipocytes. PPAR Res 2013;2013:476049.
[22] Barbera MJ, Schluter A, Pedraza N, Iglesias R, Villarroya F, Giralt M. Peroxisome proliferator-activated receptor alpha activates transcription of the brown fat uncoupling protein-1 gene. a link between regulation of the thermogenic and lipid oxidation pathways in the brown fat cell. J Biol Chem 2001;276:1486–93.
[23] Festuccia WT, Blanchard PG, Richard D, Deshaies Y. Basal adrenergic tone is required for maximal stimulation of rat brown adipose tissue UCP1 expression by chronic PPAR-gamma activation. Am J Physiol Regul Integr Comp Physiol 2010;299(1):R159–67.
[24] Fukui Y, Masui S, Osada S, Umesono K, Motojima K. A new thiazolidinedione, NC-2100, which is a weak PPAR-gamma activator, exhibits potent antidiabetic effects and induces uncoupling protein 1 in white adipose tissue of KKAy obese mice. Diabetes 2000;49(5):759–67.
[25] Bertholet AM, Kazak L, Chouchani ET, Bogaczyńska MG, Paranjpe I, Wainwright GL, Bétourné A, et al. Mitochondrial patch clamp of beige adipocytes reveals UCP1-positive and UCP1-negative cells both exhibiting futile creatine cycling. Cell Metab 2017;25(4):811–22.
[26] Friederich M, Nordquist L, Olerud J, Johansson M, Hansell P, Palm F. Identification and distribution of uncoupling protein isoforms in the normal and diabetic rat kidney. Adv Exp Med Biol 2009;645:205–12.
[27] Shabalina IG, Petrovic N, Kramarova TV, Hoeks J, Cannon B, Nedergaard J. UCP1 and defense against oxidative stress. 4-Hydroxy-2-nonenal effects on brown fat mitochondria are uncoupling protein 1-independent. J Biol Chem 2006;281:13882–93.
[28] Adjeitey CN, Mailloux RJ, Dekemp RA, Harper ME. Mitochondrial uncoupling in skeletal muscle by UCP1 augments energy expenditure and glutathione content while mitigating ros production. Am J Physiol Endocrinol Metab 2013;305(3):E405–15.
[29] Nigro M, De Sanctis C, Formisano P, Stanzione R, Forte M, Capasso G, et al. Cellular and subcellular localization of uncoupling protein 2 in the human kidney. J Mol Histol 2018;49(4):437–45.
[30] Akhmedov AT, Rybin V, Marín-García J. Mitochondrial oxidative metabolism and uncoupling proteins in the failing heart. Heart Fail Rev 2015;20(2):227–49.
[31] Jabůrek M, Ježek J, Ježek P. Cytoprotective activity of mitochondrial uncoupling protein-2 in lung and spleen. FEBS Open Bio 2018;8(4):692–701.
[32] Qin N, Cai T, Ke Q, Yuan Q, Luo J, Mao X, et al. UCP2-dependent improvement of mitochondrial dynamics protects against acute kidney injury. J Pathol 2019;247(3):392–405.
[33] Demine S, Renard P, Arnould T. Mitochondrial uncoupling: a key controller of biological processes in physiology and diseases. Cells 2019;8(8):795.
[34] Lyamzaev KG, Tokarchuk AV, Panteleeva AA, Mulkidjanian AY, Skulachev VP, Chernyak BV. Induction of autophagy by depolarization of mitochondria. Autophagy 2018;14(5):921–4.
[35] Winn NC, Vieira-Potter VJ, Gastecki ML, Welly RJ, Scroggins RJ, Zidon TM, et al. Loss of UCP1 exacerbates western diet-induced glycemic dysregulation independent of changes in body weight in female mice. Am J Physiol Regul Integr Comp Physiol 2017;312(1):R74–84.
[36] Zoladz JA, Koziel A, Woyda-Ploszczyca A, Celichowski J, Jarmuszkiewicz W. Endurance training increases the efficiency of rat skeletal muscle mitochondria. Pflugers Arch 2016;468(10):1709–24.
[37] Villarroya F, Iglesias R, Giralt M. PPARs in the control of uncoupling proteins gene expression. PPAR Res 2007;2007:74364.
[38] Kelly LJ, Vicario PP, Thompson GM, Candelore MR, Doebber TW, Ventre J, et al. Peroxisome proliferator-activated receptors gamma and alpha mediate in vivo regulation of uncoupling protein (UCP-1, UCP-2, UCP-3) gene expression. Endocrinology 1998;139(12):4920–7.